Don't blink : detecting transiting exoplanets with MASCARA

Talens, G.J.J.

Author: Talens, G.J.J.
Title: Don't blink : detecting transiting exoplanets with MASCARA
Issue Date: 2018-12-19

1 Introduction

As recently as the early 1990s, the question of whether planets existed outside our own solar system had yet to be answered. The first exoplanet detections occurred in 1992, when Wolszczan & Frail announced the discovery of two planets, a few times more massive than the earth, orbiting the pulsar PSR B1257+12 (Wolszczan and Frail, 1992). While this discovery was tantalizing, it was difficult to place it into context, as pulsars are by no means typical stars. Only a few years later, in 1995, Mayor & Queloz announced the discovery of a planet around the G-type star 51 Pegasi (Mayor and Queloz, 1995). Though this star was of ordinary solar-type, the planet was not. It has a mass about half that of Jupiter, yet it orbits its host star in only 4.23 days, far shorter than any planet in the solar system. Since the discovery of 51 Peg b the number of known exoplanets around main sequence stars has increased steadily, and several thousand exoplanets are known today. With this large number of planets the question of whether extrasolar planets exist has been definitively answered, yet the large range of observed exoplanet types has raised many new questions, such as how the observed planets formed, how they subsequently evolved and whether some of them could be habitable. In this introduction I will first provide a brief overview of the methods used to detect exoplanets. Subsequently, I discuss what we can learn about these planets and how this thesis contributes to answering the general science questions above.

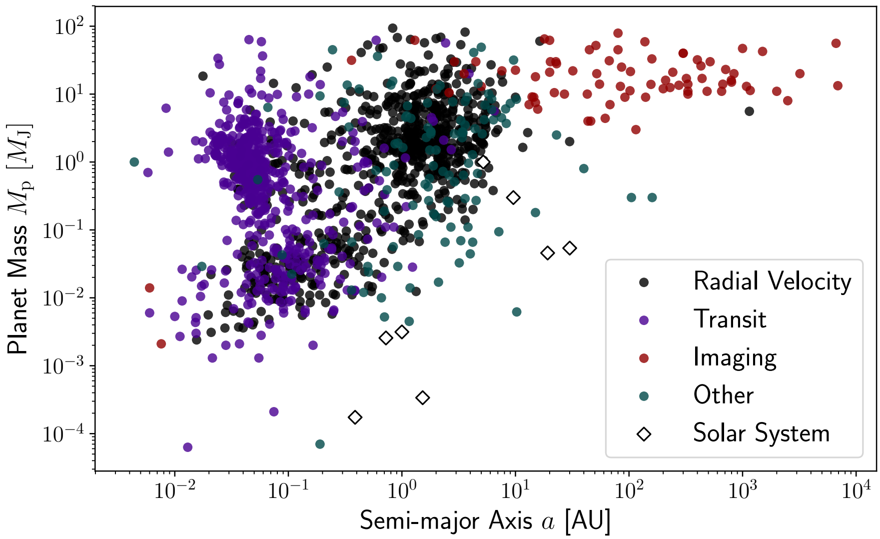

Figure 1.1: Planet mass versus orbital semi-major axis for all planets discovered to date. Extrasolar planets are marked with circles and coloured according to the method used in the detection of the exoplanet. The large diamonds indicate the solar system planets.

1.1 Detecting planets

The discovery of a planet around 51 Pegasi gave a strong impulse to the detection of extrasolar planets. Over the subsequent 20 years the number of detected exoplanets grew exponentially. At first planets were primarily detected through the radial velocity method, the same way 51 Peg b had been found. Starting in the early 2000s the transit method yielded its first detections, and is the most successful detection method today. Both the radial velocity and transit methods lack sensitivity to planets at larger separations ($>$1 AU), motivating the use of direct imaging as an exoplanet detection method in recent years.

Figure 1.1 shows the planet mass versus the orbital semi-major axis for all known exoplanets. They are coloured according to their detection method and the regions of parameters space where the different methods are most sensitive are clearly visible. Radial velocities are currently sensitive to planets out to about $\sim$5 AU, transits perform best at smaller semi-major axes, and direct imaging can detect planets out to very large separations.

1.1.1 Radial velocities and transits

Radial velocities are measured from shifts of spectral lines in the stellar spectrum, which are caused by the Doppler effect as the star orbits the center of mass of the star-planet system. For a circular orbit the observed radial velocity amplitude (K) is given by,

$$K = \left(\frac{2\pi G}{P}\right)^{1/3} \frac{M_{\rm p} \sin i}{(M_\star + M_{\rm p})^{2/3}} \tag{1.1}$$

where G is the gravitational constant, P the orbital period, $M_{\rm p}$ the mass of the planet, $M_\star$ the mass of the star, and i the inclination of the orbit relative to the observer's line of sight (e.g. Perryman, 2014). Radial velocity surveys are biased towards massive planets with short orbital periods as these produce the strongest signals. This explains why planets detected at larger separations tend to be more massive (see Fig. 1.1). Note that in most cases the true mass of a planet cannot be determined, only a lower limit, due to the unknown inclination.

Radial velocity surveys (e.g. Vogt et al., 2000; Mayor et al., 2003; Valenti and Fischer, 2005; Covino et al., 2013) generally require many observations per star over a long period of time, hence surveys tend to focus on small samples of spectroscopically well-behaved stars. Early-type stars (such as A-stars) are typically excluded from radial velocity surveys because they rotate rapidly, which broadens the spectral lines, exhibit pulsations, and have a reduced number of strong metal lines compared to solar-type stars, significantly reducing the accuracy with which radial velocities can be measured.

Soon after the discovery of the first exoplanets it was realised that for favourable inclinations, a planet would transit its host star. Detection of such transits, combined with radial velocity measurements, would allow for measurements of the true mass and radius of the planet. During a transit the planet passes in front of its host star, obscuring part of the star and causing a measurable decrease in brightness. The change in the measured flux (ΔF) relative to the out-of-transit flux (F) is proportional to the fraction of the stellar disk blocked by the planet,

$$\frac{\Delta F}{F} = \left(\frac{R_{\rm p}}{R_\star}\right)^2$$

where $R_{\rm p}$ is the radius of the planet and $R_\star$ the radius of the star. The quantity $\Delta F/F$ is usually referred to as the transit depth. Transit surveys are biased towards relatively large planets as these produce deeper transits. Furthermore, the probability that a given orbital configuration exhibits transits decreases as the semi-major axis increases, introducing a bias for smaller separations, in addition to the fact that transits occur more frequently for planets with shorter orbital periods.

The first planet to be observed in transit was HD 209458 b (Henry et al., 2000; Charbonneau et al., 2000), which was discovered using radial velocity measurements, constraining the mass and radius of the planet to $0.69\ M_{\rm J}$ and $1.38\ R_{\rm J}$. Subsequently, Charbonneau et al. (2002) showed that sodium could be detected in the atmosphere of HD 209458 b during transit, solidifying the value of transiting exoplanets for planetary characterization.

Recognizing the value of transiting exoplanets, the first ground-based transit surveys were initiated, and in 2003 the successful detection of OGLE-TR-56 b was reported (Konacki et al., 2003). Since then several ground-based transit surveys have contributed to the detection of new transiting exoplanets, such as TrES and XO (Alonso et al., 2004; McCullough et al., 2005), which found five and six planets respectively. The most successful ground-based surveys to date are HATNet and SuperWASP (Bakos et al., 2004; Pollacco et al., 2006), which in over a decade of operations have found a total of $\sim$200 exoplanets. To achieve this, HATNet and SuperWASP use a battery of wide-field lenses to target stars with magnitudes typically in the range $10 < m_V < 13$, which ensures a sufficiently large number of stars are within the Field-of-View (FoV) of the cameras. Though targeted at fainter stars, HATNet and SuperWASP have found planets orbiting the significantly brighter stars HAT-P-2 ($m_V = 8.3$) and WASP-33 ($m_V = 8.7$) (Bakos et al., 2007; Collier Cameron et al., 2010). More recently, the KELT survey (Pepper et al., 2007) has targeted brighter stars $8 < m_V < 11$, with the brightest planet hosts discovered being KELT-11 ($m_V = 8.0$) and KELT-9 ($m_V = 7.6$) (Pepper et al., 2017; Gaudi et al., 2017), and is the closest comparison to MASCARA - the subject of this thesis.

Though successful, the Earth's atmosphere limits the precision achievable with ground-based instruments, preventing the detection of smaller planets - at least around solar-type stars. In order to overcome this limitation the CoRoT (Barge et al., 2008) and *Kepler* (Borucki et al., 2010) satellites performed transit surveys from space, leading to discoveries of the first rocky Earth-size planets (Léger et al., 2009; Batalha et al., 2011). CoRoT observed several $4\ \mathrm{deg}^2$ fields for 150 days, each field containing $5000 - 10000$ stars, however its relatively short time-baseline prevented it from targeting planets in Earth-like orbits. *Kepler* observed a single $115\ \mathrm{deg}^2$ field, containing 150,000 stars, for 4 years. In this way *Kepler* found thousands of exoplanets and was able to push towards the detection of planets in Earth-like orbits. Unfortunately, most of the CoRoT and *Kepler* planet host stars are too faint ($m_V \gtrsim 13$) for follow-up measurements intended to characterise the detected planets.

1.1.2 Direct imaging and other methods

Several other methods for detecting exoplanets exist, direct imaging, pulsar timing, astrometry, microlensing, and transit-timing variations. Of these methods, direct imaging is arguably the most promising. Direct imaging is currently most sensitive to planets on wider orbits ($a \gtrsim 10$ AU), complementing the radial velocity and transit methods. As the name suggests it aims to observe the planet directly, rather then by its indirect effect on the host star. The main challenge is suppressing the light of the host star, which for Earth-like planets (in reflected light) is a factor $>10^9$ brighter at visible wavelegths. To remove the stellar light coronagraphs are used, which block or attenuate the light coming from the star, allowing for the detection of the faint signals produced by planetary companions. For ground-based telescopes coronagraphs need to be operated in conjunction with adaptive optics, which correct for aberrations due to Earth's atmosphere. Currently, direct imaging is limited to young planetary systems for which the planets still radiate residual heat from their formation, making the infrared star-to-planet contrast significantly more favourable (Chabrier et al., 2000; Burrows et al., 2004).

Pulsar timing measures the orbit of the host star as induced by the planet, similar to the radial velocity method, but by measuring the change in arrival times of the radiation pulses these objects produce. As mentioned earlier this method was actually the first to successfully detect exoplanets, but pulsars are exotic host stars and only a few more planets have been found this way. It is not clear how these planets could have survived the preceding supernova, and they may actually have formed in the wake of the explosion. Astrometry aims to measure the orbit of the host star through accurate measurements of its position on the sky. The high accuracy and frequent measurements needed have prevented large scale success with this method, however the *Gaia* mission (Gaia Collaboration et al., 2016) is very promising in this respect, and is expected to find several thousand exoplanets (Perryman et al., 2014; Snellen and Brown, 2018). Microlensing measures the change that occurs when a planetary system passes in front of a more distant star, acting as a lens to the distant star and causing it to appear brighter. Interestingly, it is also sensitive to planets that do not orbit a star, so-called free-floating planets (Han et al., 2004). However, measurements with this technique cannot be repeated, as it relies on a favourable alignment with a background star (Gaudi, 2012). Finally, transit-timing variations can be used to detect additional planets in systems where other transiting planets are known. In such a system, additional planets would modify the orbit of the known planet, changing the time at which the transit occurs by a small amount. If these transit-times can be measured for a sufficient number of orbits, additional planets can be identified even if they do not transit the host stars themselves. As this technique requires many transits and accurate transit-times, it has been most successful with the *Kepler* data (e.g. Holman et al., 2010; Steffen et al., 2013).

1.2 Hot Jupiters

Today, a wide variety of exoplanets has been discovered, from small rocky planets to massive gas giant planets. Many of these planets have no close analogues in the solar system, e.g. with particularly close-in or very wide orbits, or with intermediate masses between Earth and Neptune. One such class of planets are the hot Jupiters. They are gas giant planets with masses $0.3 - 13.6\ M_{\rm J}$ and ultra-short orbital periods <10 days - compared to that of Mercury of ∼88 days. The first exoplanet discovered, 51 Peg b, is such a hot Jupiter. They are the easiest class of object to find in transit and radial velocity surveys due to the strong observational biases.

Hot Jupiters are some of the most extreme planets known. As a result of their short orbital distances they are expected to receive high levels of irradiation and be tidally locked. The most extreme planets have day-side temperatures as hot as the effective temperatures of the coolest stars. Contrary to stars however, hot Jupiters are externally heated, making the structure of their atmospheres very different from that of stars. Their high temperatures make hot Jupiters extremely well suited for studies aimed at characterizing their atmospheres, as the temperature increases the scale-height of the atmosphere and thus the amplitude of the expected signal. The overarching scientific questions of exoplanet characterisation can be categorised around three topics: on their formation, their evolution, and possible habitability. Observational avenues that can be used to start to address these topics are orbital configurations, occurrence rates (as a function of mass and orbit), compositional constraints, and atmospheric studies.

1.2.1 Orbits, occurrence and composition

One of the first parameters that can be measured for the majority of newly discovered exoplanets is the orbital period. Precise radial velocity observations can additionally determine the eccentricity of the orbit, and its inclination can be constrained if the planet transits. Hot Jupiters are likely formed at much wider separations before migrating inward (Mizuno, 1980; Pollack et al., 1996). It is also found that most hot Jupiters are in circular

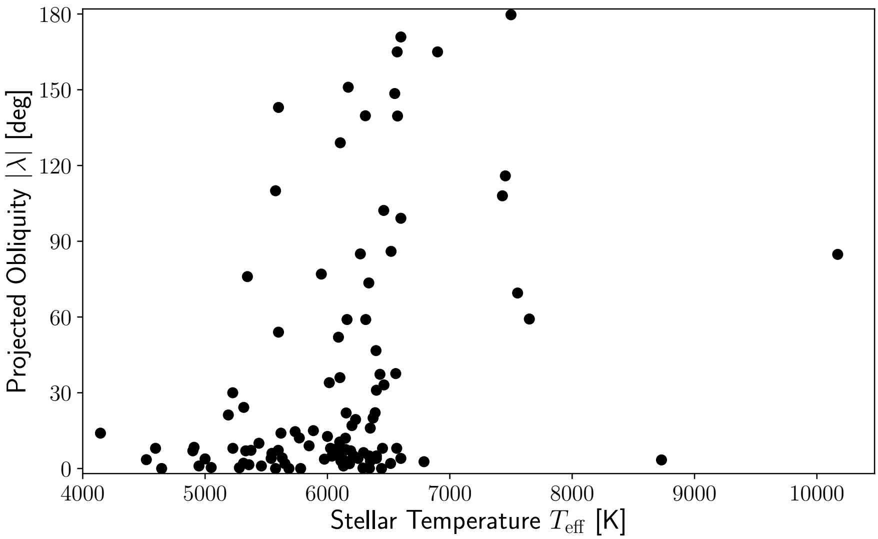

Figure 1.2: Obliquity versus stellar effective temperature for exoplanets. At $T_{\rm eff} \lesssim 6250$ K the obliquities are close to $0°$ as expected from planet formation theories. At higher temperatures the distribution is more random, suggesting some process modifies the alignment during the formation or evolution of planets around hot stars.

orbits ($e \sim 0$), which is expected due to circularization from tidal interaction with their host stars. The same mechanism should synchronise their spin-rotation with the orbital period on short time scales, tidally locking the planets (Mazeh, 2008; Goldreich and Soter, 1966).

For transiting hot Jupiters, measurements of the Rossiter-McLaughlin effect can be obtained, constraining the projected spin-orbit alignment. When the planet transits it blocks part of the rotating surface of the star, altering the stellar line profile in a way that depends on the angle between the plane of the planet orbit and the spin-rotation axis of the star (λ). Star and planet formation theory suggests that planets form in disks of gas and dust around their host stars. These disks rotate around the star and it is expected that the plane of the disk will be perpendicular to the rotation axis of the star. From this it follows that the orbital plane of the planet should also be perpendicular to the stellar rotation axis, giving $\lambda = 0°$. Figure 1.2 shows the known obliquities as a function of the stellar effective temperature ($T_{\rm eff}$). For stars with $T_{\rm eff} \lesssim 6250$ K, the measurements do indeed cluster near $0°$, however at higher temperatures they appear to be randomly distributed. This difference suggest that for planets around hotter stars a process alters the spin-orbit alignment during either their formation or evolution (Winn et al., 2010; Albrecht et al., 2012). However, only a handful of measurements exist for hotter stars, and more obliquity measurements for planets around hot stars are required to confirm the trend and distinguish between proposed causes for the misalignment, such as gravitational interactions with other stars or planets in the system[1].

From the detected population of planets (see Fig. 1.1) occurrence rates may be deter-

[1]The possible causes of spin-orbit misalignment are listed in Sect. 4.5

mined, showing how likely a star is to posses a planet, what types of planets are more common, and whether this depends on the properties of the host stars. Batalha (2014), drawing from several occurrence rate studies, concluded that late-type main sequence stars are orbited by at least one planet. Though hot Jupiters are the most common type of planet detected by ground-based radial velocity and transit surveys, their occurrence rate is actually only $\sim$1% (Mayor et al., 2011; Wright et al., 2012; Howard et al., 2012; Fressin et al., 2013). The high discovery rate of hot Jupiters detected is a result of the biases discussed in Sect. 1.1, rather than the true population of planets.

From combining transit and radial velocity measurements the planet mass and radius are obtained, constraining the bulk density of the planet, allowing inferences to be made about the composition of exoplanets. Like Jupiter and Saturn, hot Jupiters are expected to have a low density as they should be primarily composed of H and He. Figure 1.3 shows the radius versus mass for hot Jupiters, coloured by the equilibrium temperature of the planet. The solid black line indicates the expected relation between the mass and radius of a 3 Gyr old gas giant planet at 0.045 AU from the Sun. It is clear that many hot Jupiters have larger radii and thus lower densities than expected from a H/He composition, a result that holds even when accounting for variations in age and metallicity (Baraffe et al., 2008). This inflation might be related to the amount of flux they receive from their host star, as the most inflated planets also have the highest temperatures. There are several theories that attempt to explain the cause for these inflated radii, either by including an internal heating source (Bodenheimer et al., 2001; Miller et al., 2009; Batygin and Stevenson, 2010; Wu and Lithwick, 2013) or by slowing down the cooling and contraction of the planet during its evolution (Guillot and Showman, 2002; Burrows et al., 2007; Perna et al., 2010), but no definite answer has been identified yet.

1.2.2 Atmospheres

Much work has been done on characterising the atmospheric properties of exoplanets. The atmospheres of transiting exoplanets can be investigated using secondary eclipse measurements, by means of phase curve observations, and through transmission spectroscopy. During secondary eclipse the star blocks thermal emission and reflected light coming from the planet. Measuring this decrease in brightness using broadband photometry places constraints on the day-side temperature of the planet and the reflectivity, or albedo, of its atmosphere. In addition, spectra of the planet may be obtained by taking the difference between those obtained just before or after the eclipse, when both the star and planet contribute, and during the eclipse, containing only the star. Phase curves measure the change in brightness due to changes in the visible fraction of the planet day-side over the course of the orbit. From phase curve measurements the contrast between the planet's day- and night-side can be constrained, and the time of maximum brightness contains information on the dynamics of the atmosphere. Transmission spectroscopy measures small variations in the transit depth with wavelength, which are caused by changes in the optical depth of the atmosphere and can thus be interpreted as a spectrum.

The first detection of an exoplanet atmosphere was made by Charbonneau et al. (2002) who showed sodium was present in the atmosphere of the hot Jupiter HD 209458 b, using spectra taken with the STIS spectrograph on the Hubble Space Telescope (HST). Since then the atmospheres of exoplanets have been extensively studied, from space using the

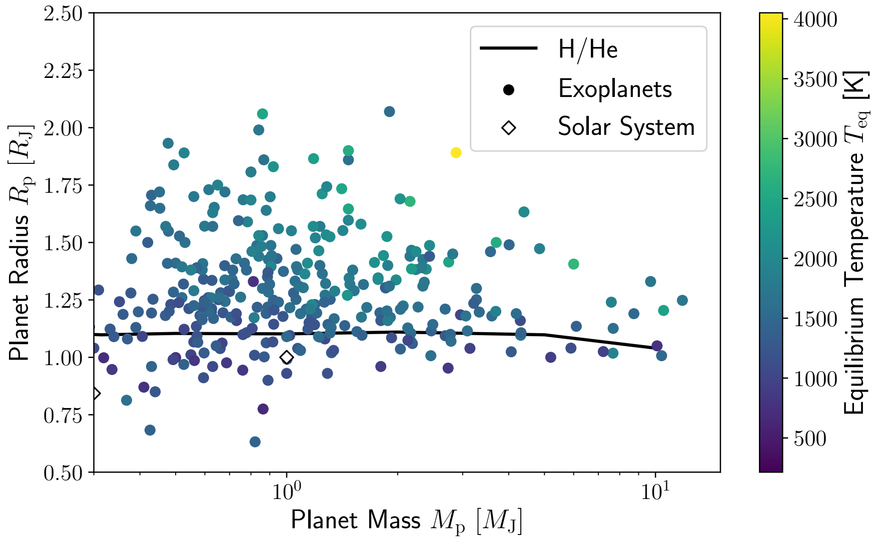

Figure 1.3: Planet mass versus planet radius, hot Jupiters are indicated by circles and solar system planets by the white diamonds. The hot Jupiters are coloured by their equilibrium temperature. The solid line, taken from Baraffe et al. (2008), indicates the mass-radius relation for a 3 Gyr year old H/He gas giant planet at 0.045 AU from the Sun.

STIS and WFC3 low-resolution spectrographs on HST and broadband photometry from *Spitzer* IRAC. STIS is an optical ($0.2 - 1$ μm) spectrograph which has been used to detect to Na and K as well as slopes due to Rayleigh scattering processes, while WFC3 in the near-infrared ($1.1 - 1.7$ μm) is primarily sensitive to H_2O, and *Spitzer* IRAC photometry places additional constraints in the far-infrared. The James Webb Space Telescope will revolutionise space-based spectroscopy of exoplanets by providing spectral coverage from $0.6 - 28$ μm (Beichman et al., 2014), it is currently set for launch in 2021, though Munroe (2018) predicts a 2026 launch.

From photometry and low-resolution spectroscopy it has been found that hot Jupiters have low albedos (Schwartz and Cowan, 2015). Due to tidal locking they often have high day-side temperatures and large day/night-side contrasts (Komacek et al., 2017). For many hot Jupiters it has also been found that their transit spectra contain no significant spectral features, indicative of high-altitude clouds and hazes blocking radiation coming from deeper layers of the atmospheres (e.g. Sing et al., 2016). Measurements of the atomic and molecular species present in hot Jupiter atmospheres could provide information on their formation. The C/O ratio in particular is thought to be a tracer of formation location in the protoplanetary disk (Öberg et al., 2011). Furthermore, the strong stellar irradiation hot Jupiters receive could cause inversions in the temperature structure of the atmosphere, if strong absorbers such as TiO or VO are present. Recently, the first robust evidence for the existence of thermal inversions was obtained when TiO was detected in the atmospheres of two hot Jupiters (Nugroho et al., 2017; Sedaghati et al., 2017).

In addition to the observations performed with space-based instrumentation, Snellen et al. (2010) showed that high resolution ground-based spectroscopy can be effectively used to unambiguously identify molecular species, such as CO in the atmosphere of HD 209458 b, using cross-correlating techniques, targeting the many spectral molecular lines providing a unique fingerprint for a molecule. Since then, high-resolution spectroscopy has been used to infer the presence of CO, H_2O, TiO HCN, Fe, Fe^+ and Ti^+ in the atmospheres of hot Jupiters (e.g. Birkby et al., 2013; de Kok et al., 2013; Rodler et al., 2013; Nugroho et al., 2017; Hawker et al., 2018; Hoeijmakers et al., 2018). Once a molecule has been detected at high-resolution the shape and location of the cross-correlation profile provide additional information. It has been used to measure winds in the atmospheres of HD 209458 b and HD 189733 b (Snellen et al., 2010; Brogi et al., 2016), measure true masses for the non-transiting planets τ Boo b, HD 88138 b, ups And b and 51 Peg b (Brogi et al., 2012; Rodler et al., 2012; Lockwood et al., 2014; Piskorz et al., 2016, 2017; Birkby et al., 2017), and constrain the rotation rates of β Pic b, HD 189733 b and GQ Lupi b (Snellen et al., 2014; Brogi et al., 2016; Schwarz et al., 2016).

1.3 This thesis

This thesis is focused on the construction, software development, operation, data calibration and analysis, and the first results of the Multi-site All-Sky CAmeRA (MASCARA), which aims to find transiting exoplanets orbiting the brightest stars in the sky. Although *Kepler* and CoRoT have identified thousands of transiting planets, and ground-based surveys like SuperWASP and HATNet have found hundreds of hot Jupiters, they all stay well clear of the brightest stars. However, the brightest stars are particularly interesting, because they allow for the most detailed follow-up observations - in particular for the characterisation of their atmospheres. In addition, the bright star population is biased towards early-type stars, which are strongly under-represented in both radial velocity and transit surveys because mass measurements are near-impossible at faint magnitudes (since early-type stars are fast rotators) but can be accessible at the magnitudes probed by MASCARA. Comparison of the occurrence rates as a function of orbital period and planet mass, as well as their spin-orbital alignments, can shed interesting new light on the formation processes of hot Jupiters.

With this in mind, Snellen et al. (2012) proposed an all-sky transit survey of the brightest stars in the sky ($4 < m_V < 8.4$), the Multi-site All-Sky CAmeRA (MASCARA). MASCARA now consists of two stations, one in the northern hemisphere and one in the southern hemisphere. Each station uses five cameras to image the entire local sky with a cadence of 6.4 s. The first MASCARA station, shown in Fig. 2.1, is located at the Observatorio del Roque de los Muchachos and started nominal operations in January of 2015. The second station, shown in Fig. 1.4, is located at La Silla observatory and started nominal operations in November 2017. A sister-survey called bRing (Stuik et al., 2017), built using the same optics and using the same observing cadence as MASCARA, was also constructed in 2017. bRing consists of two stations in the southern hemisphere that each use two cameras to image stars with $\delta \lesssim -30°$. The bRing stations are located at the Sutherland Observing Station and Siding Spring Observatory.

Figure 1.4: The MASCARA station located at La Silla observatory in Chile, shown during the final stages of construction in June 2017. The camera box has been opened so the lenses can be cleaned, allowing the cameras and lenses to be viewed at the top of the instrument. The camera box can be seen at the bottom of the image as the black object with circular windows. The author (right) and Gilles Otten (left) are also visible.

Chapter 2 This chapter describes the optical and mechanical design of the MASCARA stations and outlines the observational strategy used by MASCARA. Each station uses five Kodak KAI-110002 interline CCDs equipped with commercial canon lenses, giving each camera a FoV of $53° \times 74°$. The camera mounts do not correct for the rotation of the Earth, and stare at fixed points on the local sky instead, i.e. stars move across the CCDs during the observations. The choice of fixed pointings for the cameras means that the roof is the only moving element of the stations, reducing the chance of mechanical failures. The stations take synchronized exposures every 6.4 sidereal seconds, with no read-out time between exposures thanks to the interline design of the CCDs. Each station takes ~500 GB of raw exposures per night, prohibiting transfer and storage of the raw images. An on-site reduction pipeline creates astrometric solutions, performs aperture photometry and creates stacked images. These data products are transferred to Leiden for further processing.

Chapter 3 In this chapter the calibration pipeline, which is used to remove the systematic effects present in the MASCARA and bRing data, is described. The calibration pipeline had to account for systematics introduced by the motion of stars across the CCDs during the observations, a unique feature of MASCARA and bRing. The pipeline consists of a primary calibration step which uses groups of stars to remove the effects of the Earth's atmosphere, camera transmission, and intrapixel variations. Empirical secondary calibration methods are then used to remove residual trends from the photometry of individual stars. After calibration an RMS scatter of 10 mmag is achieved at $m_V \sim 7.5$. The performance of MASCARA is characterized by injecting realistic transit signals into the light curves and identifying which signals can be recovered. From 1 year of data from the MASCARA station on La Palma, and injecting signals with $1 < P < 5$ days, we find 84.0%, 60.5% and 20.7% of the signals are recovered for transit depths of 2%, 1% and 0.5%, respectively. Furthermore there is a strong dependence on the observed declination, as 65.4% of all transit signals are recovered at $\delta > 0°$ versus 35.8% at $\delta < 0°$. With the first discoveries of MASCARA (see Chapters 4 and 5) we also made a first attempt to constrain the occurrence rate of hot-Jupiters around A-stars.

Chapters 4 and 5 These chapters present the first scientific results of MASCARA - the detections of MASCARA-1 b and MASCARA-2 b, two of the brightest hot Jupiter systems in the sky. MASCARA-1 b is in a 2.15 day orbit around the A-type star HD 201585 ($m_V = 8.3$). The planet has a radius of $1.5\ R_\mathrm{J}$ and a mass of $3.7\ M_\mathrm{J}$. The high temperature of its host star ($T_\mathrm{eff} = 7554$ K) and its close-in orbit ($a = 0.043$ AU) give MASCARA-1 b a high equilibrium temperature of 2570 K, making it suitable for high-resolution spectroscopy. Like other planets around hot stars it has a high obliquity, $\lambda = 69.5°$, apparently confirming the trend of planets around hot stars preferring misaligned orbits. MASCARA-2 b is in a 3.75 day orbit around the A-type star HD 185603 ($m_V = 7.6$). The planet has a radius of $1.83\ R_\mathrm{J}$ and a mass $<17\ M_\mathrm{J}$. Though not as hot as MASCARA-1 b, it nevertheless has a high equilibrium temperature of 2260 K, making it very suitable for high-resolution spectroscopy. Contrary to other planets around hot stars it has a low obliquity, $\lambda = 0.6°$, making it the first planet around a star with $T_\mathrm{eff} > 7000$ K whose orbit is perpendicular to the stellar spin axis.

Bibliography

Albrecht, S., Winn, J. N., Johnson, J. A., Howard, A. W., Marcy, G. W., Butler, R. P., Arriagada, P., Crane, J. D., Shectman, S. A., Thompson, I. B., Hirano, T., Bakos, G., and Hartman, J. D. (2012). Obliquities of Hot Jupiter Host Stars: Evidence for Tidal Interactions and Primordial Misalignments. *ApJ*, 757:18.

Alonso, R., Brown, T. M., Torres, G., Latham, D. W., Sozzetti, A., Mandushev, G., Belmonte, J. A., Charbonneau, D., Deeg, H. J., Dunham, E. W., O'Donovan, F. T., and Stefanik, R. P. (2004). TrES-1: The Transiting Planet of a Bright K0 V Star. *ApJ*, 613:L153–L156.

Bakos, G., Noyes, R. W., Kovács, G., Stanek, K. Z., Sasselov, D. D., and Domsa, I. (2004). Wide-Field Millimagnitude Photometry with the HAT: A Tool for Extrasolar Planet Detection. *PASP*, 116:266–277.

Bakos, G. Á., Kovács, G., Torres, G., Fischer, D. A., Latham, D. W., Noyes, R. W., Sasselov, D. D., Mazeh, T., Shporer, A., Butler, R. P., Stefanik, R. P., Fernández, J. M., Sozzetti, A., Pál, A., Johnson, J., Marcy, G. W., Winn, J. N., Sipőcz, B., Lázár, J., Papp, I., and Sári, P. (2007). HD 147506b: A Supermassive Planet in an Eccentric Orbit Transiting a Bright Star. *ApJ*, 670:826–832.

Baraffe, I., Chabrier, G., and Barman, T. (2008). Structure and evolution of super-Earth to super-Jupiter exoplanets. I. Heavy element enrichment in the interior. *A&A*, 482:315–332.

Barge, P., Baglin, A., Auvergne, M., Rauer, H., Léger, A., Schneider, J., Pont, F., Aigrain, S., Almenara, J.-M., Alonso, R., Barbieri, M., Bordé, P., Bouchy, F., Deeg, H. J., La Reza, D., Deleuil, M., Dvorak, R., Erikson, A., Fridlund, M., Gillon, M., Gondoin, P., Guillot, T., Hatzes, A., Hebrard, G., Jorda, L., Kabath, P., Lammer, H., Llebaria, A., Loeillet, B., Magain, P., Mazeh, T., Moutou, C., Ollivier, M., Pätzold, M., Queloz, D., Rouan, D., Shporer, A., and Wuchterl, G. (2008). Transiting exoplanets from the CoRoT space mission. I. CoRoT-Exo-1b: a low-density short-period planet around a G0V star. *A&A*, 482:L17–L20.

Batalha, N. M. (2014). Exploring exoplanet populations with NASA's Kepler Mission. *Proceedings of the National Academy of Science*, 111:12647–12654.

Batalha, N. M., Borucki, W. J., Bryson, S. T., Buchhave, L. A., Caldwell, D. A., Christensen-Dalsgaard, J., Ciardi, D., Dunham, E. W., Fressin, F., Gautier, III, T. N., Gilliland, R. L., Haas, M. R., Howell, S. B., Jenkins, J. M., Kjeldsen, H., Koch, D. G., Latham, D. W., Lissauer, J. J., Marcy, G. W., Rowe, J. F., Sasselov, D. D., Seager, S., Steffen, J. H., Torres, G., Basri, G. S., Brown, T. M., Charbonneau, D., Christiansen, J., Clarke, B., Cochran,

W. D., Dupree, A., Fabrycky, D. C., Fischer, D., Ford, E. B., Fortney, J., Girouard, F. R., Holman, M. J., Johnson, J., Isaacson, H., Klaus, T. C., Machalek, P., Moorehead, A. V., Morehead, R. C., Ragozzine, D., Tenenbaum, P., Twicken, J., Quinn, S., VanCleve, J., Walkowicz, L. M., Welsh, W. F., Devore, E., and Gould, A. (2011). Kepler's First Rocky Planet: Kepler-10b. *ApJ*, 729:27.

Batygin, K. and Stevenson, D. J. (2010). Inflating Hot Jupiters with Ohmic Dissipation. *ApJ*, 714:L238–L243.

Beichman, C., Benneke, B., Knutson, H., Smith, R., Lagage, P.-O., Dressing, C., Latham, D., Lunine, J., Birkmann, S., Ferruit, P., Giardino, G., Kempton, E., Carey, S., Krick, J., Deroo, P. D., Mandell, A., Ressler, M. E., Shporer, A., Swain, M., Vasisht, G., Ricker, G., Bouwman, J., Crossfield, I., Greene, T., Howell, S., Christiansen, J., Ciardi, D., Clampin, M., Greenhouse, M., Sozzetti, A., Goudfrooij, P., Hines, D., Keyes, T., Lee, J., McCullough, P., Robberto, M., Stansberry, J., Valenti, J., Rieke, M., Rieke, G., Fortney, J., Bean, J., Kreidberg, L., Ehrenreich, D., Deming, D., Albert, L., Doyon, R., and Sing, D. (2014). Observations of Transiting Exoplanets with the James Webb Space Telescope (JWST). *PASP*, 126:1134.

Birkby, J. L., de Kok, R. J., Brogi, M., de Mooij, E. J. W., Schwarz, H., Albrecht, S., and Snellen, I. A. G. (2013). Detection of water absorption in the day side atmosphere of HD 189733 b using ground-based high-resolution spectroscopy at 3.2 μm. *MNRAS*, 436:L35–L39.

Birkby, J. L., de Kok, R. J., Brogi, M., Schwarz, H., and Snellen, I. A. G. (2017). Discovery of Water at High Spectral Resolution in the Atmosphere of 51 Peg b. *AJ*, 153:138.

Bodenheimer, P., Lin, D. N. C., and Mardling, R. A. (2001). On the Tidal Inflation of Short-Period Extrasolar Planets. *ApJ*, 548:466–472.

Borucki, W. J., Koch, D., Basri, G., Batalha, N., Brown, T., Caldwell, D., Caldwell, J., Christensen-Dalsgaard, J., Cochran, W. D., DeVore, E., Dunham, E. W., Dupree, A. K., Gautier, T. N., Geary, J. C., Gilliland, R., Gould, A., Howell, S. B., Jenkins, J. M., Kondo, Y., Latham, D. W., Marcy, G. W., Meibom, S., Kjeldsen, H., Lissauer, J. J., Monet, D. G., Morrison, D., Sasselov, D., Tarter, J., Boss, A., Brownlee, D., Owen, T., Buzasi, D., Charbonneau, D., Doyle, L., Fortney, J., Ford, E. B., Holman, M. J., Seager, S., Steffen, J. H., Welsh, W. F., Rowe, J., Anderson, H., Buchhave, L., Ciardi, D., Walkowicz, L., Sherry, W., Horch, E., Isaacson, H., Everett, M. E., Fischer, D., Torres, G., Johnson, J. A., Endl, M., MacQueen, P., Bryson, S. T., Dotson, J., Haas, M., Kolodziejczak, J., Van Cleve, J., Chandrasekaran, H., Twicken, J. D., Quintana, E. V., Clarke, B. D., Allen, C., Li, J., Wu, H., Tenenbaum, P., Verner, E., Bruhweiler, F., Barnes, J., and Prsa, A. (2010). Kepler Planet-Detection Mission: Introduction and First Results. *Science*, 327:977.

Brogi, M., de Kok, R. J., Albrecht, S., Snellen, I. A. G., Birkby, J. L., and Schwarz, H. (2016). Rotation and Winds of Exoplanet HD 189733 b Measured with High-dispersion Transmission Spectroscopy. *ApJ*, 817:106.

Brogi, M., Snellen, I. A. G., de Kok, R. J., Albrecht, S., Birkby, J., and de Mooij, E. J. W. (2012). The signature of orbital motion from the dayside of the planet τ Boötis b. *Nature* , 486:502–504.

Burrows, A., Hubeny, I., Budaj, J., and Hubbard, W. B. (2007). Possible Solutions to the Radius Anomalies of Transiting Giant Planets. *ApJ*, 661:502–514.

Burrows, A., Sudarsky, D., and Hubeny, I. (2004). Spectra and Diagnostics for the Direct Detection of Wide-Separation Extrasolar Giant Planets. *ApJ*, 609:407–416.

Chabrier, G., Baraffe, I., Allard, F., and Hauschildt, P. (2000). Evolutionary Models for Very Low-Mass Stars and Brown Dwarfs with Dusty Atmospheres. *ApJ*, 542:464–472.

Charbonneau, D., Brown, T. M., Latham, D. W., and Mayor, M. (2000). Detection of Planetary Transits Across a Sun-like Star. *ApJ*, 529:L45–L48.

Charbonneau, D., Brown, T. M., Noyes, R. W., and Gilliland, R. L. (2002). Detection of an Extrasolar Planet Atmosphere. *ApJ*, 568:377–384.

Collier Cameron, A., Guenther, E., Smalley, B., McDonald, I., Hebb, L., Andersen, J., Augusteijn, T., Barros, S. C. C., Brown, D. J. A., Cochran, W. D., Endl, M., Fossey, S. J., Hartmann, M., Maxted, P. F. L., Pollacco, D., Skillen, I., Telting, J., Waldmann, I. P., and West, R. G. (2010). Line-profile tomography of exoplanet transits - II. A gas-giant planet transiting a rapidly rotating A5 star. *MNRAS*, 407:507–514.

Covino, E., Esposito, M., Barbieri, M., Mancini, L., Nascimbeni, V., Claudi, R., Desidera, S., Gratton, R., Lanza, A. F., Sozzetti, A., Biazzo, K., Affer, L., Gandolfi, D., Munari, U., Pagano, I., Bonomo, A. S., Collier Cameron, A., Hébrard, G., Maggio, A., Messina, S., Micela, G., Molinari, E., Pepe, F., Piotto, G., Ribas, I., Santos, N. C., Southworth, J., Shkolnik, E., Triaud, A. H. M. J., Bedin, L., Benatti, S., Boccato, C., Bonavita, M., Borsa, F., Borsato, L., Brown, D., Carolo, E., Ciceri, S., Cosentino, R., Damasso, M., Faedi, F., Martínez Fiorenzano, A. F., Latham, D. W., Lovis, C., Mordasini, C., Nikolov, N., Poretti, E., Rainer, M., Rebolo López, R., Scandariato, G., Silvotti, R., Smareglia, R., Alcalá, J. M., Cunial, A., Di Fabrizio, L., Di Mauro, M. P., Giacobbe, P., Granata, V., Harutyunyan, A., Knapic, C., Lattanzi, M., Leto, G., Lodato, G., Malavolta, L., Marzari, F., Molinaro, M., Nardiello, D., Pedani, M., Prisinzano, L., and Turrini, D. (2013). The GAPS programme with HARPS-N at TNG. I. Observations of the Rossiter-McLaughlin effect and characterisation of the transiting system Qatar-1. *A&A*, 554:A28.

de Kok, R. J., Brogi, M., Snellen, I. A. G., Birkby, J., Albrecht, S., and de Mooij, E. J. W. (2013). Detection of carbon monoxide in the high-resolution day-side spectrum of the exoplanet HD 189733b. *A&A*, 554:A82.

Fressin, F., Torres, G., Charbonneau, D., Bryson, S. T., Christiansen, J., Dressing, C. D., Jenkins, J. M., Walkowicz, L. M., and Batalha, N. M. (2013). The False Positive Rate of Kepler and the Occurrence of Planets. *ApJ*, 766:81.

Gaia Collaboration, Prusti, T., de Bruijne, J. H. J., Brown, A. G. A., Vallenari, A., Babusiaux, C., Bailer-Jones, C. A. L., Bastian, U., Biermann, M., Evans, D. W., and et al. (2016). The Gaia mission. *A&A*, 595:A1.

Gaudi, B. S. (2012). Microlensing Surveys for Exoplanets. *ARA&A*, 50:411–453.

Gaudi, B. S., Stassun, K. G., Collins, K. A., Beatty, T. G., Zhou, G., Latham, D. W., Bieryla, A., Eastman, J. D., Siverd, R. J., Crepp, J. R., Gonzales, E. J., Stevens, D. J., Buchhave, L. A., Pepper, J., Johnson, M. C., Colon, K. D., Jensen, E. L. N., Rodriguez, J. E., Bozza, V., Novati, S. C., D'Ago, G., Dumont, M. T., Ellis, T., Gaillard, C., Jang-Condell, H., Kasper, D. H., Fukui, A., Gregorio, J., Ito, A., Kielkopf, J. F., Manner, M., Matt, K., Narita, N., Oberst, T. E., Reed, P. A., Scarpetta, G., Stephens, D. C., Yeigh, R. R., Zambelli, R., Fulton, B. J., Howard, A. W., James, D. J., Penny, M., Bayliss, D., Curtis, I. A., Depoy, D. L., Esquerdo, G. A., Gould, A., Joner, M. D., Kuhn, R. B., Labadie-Bartz, J., Lund, M. B., Marshall, J. L., McLeod, K. K., Pogge, R. W., Relles, H., Stockdale, C., Tan, T. G., Trueblood, M., and Trueblood, P. (2017). A giant planet undergoing extreme-ultraviolet irradiation by its hot massive-star host. *Nature* , 546:514–518.

Goldreich, P. and Soter, S. (1966). Q in the Solar System. *Icarus*, 5:375–389.

Guillot, T. and Showman, A. P. (2002). Evolution of "51 Pegasus b-like" planets. *A&A*, 385:156–165.

Han, C., Chung, S.-J., Kim, D., Park, B.-G., Ryu, Y.-H., Kang, S., and Lee, D. W. (2004). Gravitational Microlensing: A Tool for Detecting and Characterizing Free-Floating Planets. *ApJ*, 604:372–378.

Hawker, G. A., Madhusudhan, N., Cabot, S. H. C., and Gandhi, S. (2018). Evidence for Multiple Molecular Species in the Hot Jupiter HD 209458b. *ApJ*, 863:L11.

Henry, G. W., Marcy, G. W., Butler, R. P., and Vogt, S. S. (2000). A Transiting "51 Peg-like" Planet. *ApJ*, 529:L41–L44.

Hoeijmakers, H. J., Ehrenreich, D., Heng, K., Kitzmann, D., Grimm, S. L., Allart, R., Deitrick, R., Wyttenbach, A., Oreshenko, M., Pino, L., Rimmer, P. B., Molinari, E., and Di Fabrizio, L. (2018). Atomic iron and titanium in the atmosphere of the exoplanet KELT-9b. *Nature* , 560:453–455.

Holman, M. J., Fabrycky, D. C., Ragozzine, D., Ford, E. B., Steffen, J. H., Welsh, W. F., Lissauer, J. J., Latham, D. W., Marcy, G. W., Walkowicz, L. M., Batalha, N. M., Jenkins, J. M., Rowe, J. F., Cochran, W. D., Fressin, F., Torres, G., Buchhave, L. A., Sasselov, D. D., Borucki, W. J., Koch, D. G., Basri, G., Brown, T. M., Caldwell, D. A., Charbonneau, D., Dunham, E. W., Gautier, T. N., Geary, J. C., Gilliland, R. L., Haas, M. R., Howell, S. B., Ciardi, D. R., Endl, M., Fischer, D., Fürész, G., Hartman, J. D., Isaacson, H., Johnson, J. A., MacQueen, P. J., Moorhead, A. V., Morehead, R. C., and Orosz, J. A. (2010). Kepler-9: A System of Multiple Planets Transiting a Sun-Like Star, Confirmed by Timing Variations. *Science*, 330:51.

Howard, A. W., Marcy, G. W., Bryson, S. T., Jenkins, J. M., Rowe, J. F., Batalha, N. M., Borucki, W. J., Koch, D. G., Dunham, E. W., Gautier, III, T. N., Van Cleve, J., Cochran, W. D., Latham, D. W., Lissauer, J. J., Torres, G., Brown, T. M., Gilliland, R. L., Buchhave, L. A., Caldwell, D. A., Christensen-Dalsgaard, J., Ciardi, D., Fressin, F., Haas, M. R., Howell, S. B., Kjeldsen, H., Seager, S., Rogers, L., Sasselov, D. D., Steffen, J. H., Basri, G. S., Charbonneau, D., Christiansen, J., Clarke, B., Dupree, A., Fabrycky, D. C., Fischer, D. A., Ford, E. B., Fortney, J. J., Tarter, J., Girouard, F. R., Holman, M. J., Johnson, J. A., Klaus, T. C., Machalek, P., Moorhead, A. V., Morehead, R. C., Ragozzine, D., Tenenbaum, P., Twicken, J. D., Quinn, S. N., Isaacson, H., Shporer, A., Lucas, P. W., Walkowicz, L. M., Welsh, W. F., Boss, A., Devore, E., Gould, A., Smith, J. C., Morris, R. L., Prsa, A., Morton, T. D., Still, M., Thompson, S. E., Mullally, F., Endl, M., and MacQueen, P. J. (2012). Planet Occurrence within 0.25 AU of Solar-type Stars from Kepler. *ApJS*, 201:15.

Komacek, T. D., Showman, A. P., and Tan, X. (2017). Atmospheric Circulation of Hot Jupiters: Dayside-Nightside Temperature Differences. II. Comparison with Observations. *ApJ*, 835:198.

Konacki, M., Torres, G., Jha, S., and Sasselov, D. D. (2003). An extrasolar planet that transits the disk of its parent star. *Nature* , 421:507–509.

Léger, A., Rouan, D., Schneider, J., Barge, P., Fridlund, M., Samuel, B., Ollivier, M., Guenther, E., Deleuil, M., Deeg, H. J., Auvergne, M., Alonso, R., Aigrain, S., Alapini, A., Almenara, J. M., Baglin, A., Barbieri, M., Bruntt, H., Bordé, P., Bouchy, F., Cabrera, J., Catala, C., Carone, L., Carpano, S., Csizmadia, S., Dvorak, R., Erikson, A., Ferraz-Mello, S., Foing, B., Fressin, F., Gandolfi, D., Gillon, M., Gondoin, P., Grasset, O., Guillot, T., Hatzes, A., Hébrard, G., Jorda, L., Lammer, H., Llebaria, A., Loeillet, B., Mayor, M., Mazeh, T., Moutou, C., Pätzold, M., Pont, F., Queloz, D., Rauer, H., Renner, S., Samadi, R., Shporer, A., Sotin, C., Tingley, B., Wuchterl, G., Adda, M., Agogu, P., Appourchaux, T., Ballans, H., Baron, P., Beaufort, T., Bellenger, R., Berlin, R., Bernardi, P., Blouin, D., Baudin, F., Bodin, P., Boisnard, L., Boit, L., Bonneau, F., Borzeix, S., Briet, R., Buey, J.-T., Butler, B., Cailleau, D., Cautain, R., Chabaud, P.-Y., Chaintreuil, S., Chiavassa, F., Costes, V., Cuna Parrho, V., de Oliveira Fialho, F., Decaudin, M., Defise, J.-M., Djalal, S., Epstein, G., Exil, G.-E., Fauré, C., Fenouillet, T., Gaboriaud, A., Gallic, A., Gamet, P., Gavalda, P., Grolleau, E., Gruneisen, R., Gueguen, L., Guis, V., Guivarc'h, V., Guterman, P., Hallouard, D., Hasiba, J., Heuripeau, F., Huntzinger, G., Hustaix, H., Imad, C., Imbert, C., Johlander, B., Jouret, M., Journoud, P., Karioty, F., Kerjean, L., Lafaille, V., Lafond, L., Lam-Trong, T., Landiech, P., Lapeyrere, V., Larqué, T., Laudet, P., Lautier, N., Lecann, H., Lefevre, L., Leruyet, B., Levacher, P., Magnan, A., Mazy, E., Mertens, F., Mesnager, J.-M., Meunier, J.-C., Michel, J.-P., Monjoin, W., Naudet, D., Nguyen-Kim, K., Orcesi, J.-L., Ottacher, H., Perez, R., Peter, G., Plasson, P., Plesseria, J.-Y., Pontet, B., Pradines, A., Quentin, C., Reynaud, J.-L., Rolland, G., Rollenhagen, F., Romagnan, R., Russ, N., Schmidt, R., Schwartz, N., Sebbag, I., Sedes, G., Smit, H., Steller, M. B., Sunter, W., Surace, C., Tello, M., Tiphène, D., Toulouse, P., Ulmer, B., Vandermarcq, O., Vergnault, E., Vuillemin, A., and Zanatta, P. (2009). Transiting exoplanets from the CoRoT space mission. VIII. CoRoT-7b: the first super-Earth with measured radius. *A&A*, 506:287–302.

Lockwood, A. C., Johnson, J. A., Bender, C. F., Carr, J. S., Barman, T., Richert, A. J. W., and Blake, G. A. (2014). Near-IR Direct Detection of Water Vapor in Tau Boötis b. *ApJ*, 783:L29.

Mayor, M., Marmier, M., Lovis, C., Udry, S., Ségransan, D., Pepe, F., Benz, W., Bertaux, J. ., Bouchy, F., Dumusque, X., Lo Curto, G., Mordasini, C., Queloz, D., and Santos, N. C.

(2011). The HARPS search for southern extra-solar planets XXXIV. Occurrence, mass distribution and orbital properties of super-Earths and Neptune-mass planets. *ArXiv e-prints*.

Mayor, M., Pepe, F., Queloz, D., Bouchy, F., Rupprecht, G., Lo Curto, G., Avila, G., Benz, W., Bertaux, J.-L., Bonfils, X., Dall, T., Dekker, H., Delabre, B., Eckert, W., Fleury, M., Gilliotte, A., Gojak, D., Guzman, J. C., Kohler, D., Lizon, J.-L., Longinotti, A., Lovis, C., Megevand, D., Pasquini, L., Reyes, J., Sivan, J.-P., Sosnowska, D., Soto, R., Udry, S., van Kesteren, A., Weber, L., and Weilenmann, U. (2003). Setting New Standards with HARPS. *The Messenger*, 114:20–24.

Mayor, M. and Queloz, D. (1995). A Jupiter-mass companion to a solar-type star. *Nature* , 378:355–359.

Mazeh, T. (2008). Observational Evidence for Tidal Interaction in Close Binary Systems. In Goupil, M.-J. and Zahn, J.-P., editors, *EAS Publications Series*, volume 29 of *EAS Publications Series*, pages 1–65.

McCullough, P. R., Stys, J. E., Valenti, J. A., Fleming, S. W., Janes, K. A., and Heasley, J. N. (2005). The XO Project: Searching for Transiting Extrasolar Planet Candidates. *PASP*, 117:783–795.

Miller, N., Fortney, J. J., and Jackson, B. (2009). Inflating and Deflating Hot Jupiters: Coupled Tidal and Thermal Evolution of Known Transiting Planets. *ApJ*, 702:1413–1427.

Mizuno, H. (1980). Formation of the Giant Planets. *Progress of Theoretical Physics*, 64:544–557.

Munroe, R. (2018). JWST Delays. *xkcd*, 2014.

Nugroho, S. K., Kawahara, H., Masuda, K., Hirano, T., Kotani, T., and Tajitsu, A. (2017). High-resolution Spectroscopic Detection of TiO and a Stratosphere in the Day-side of WASP-33b. *AJ*, 154:221.

Öberg, K. I., Murray-Clay, R., and Bergin, E. A. (2011). The Effects of Snowlines on C/O in Planetary Atmospheres. *ApJ*, 743:L16.

Pepper, J., Pogge, R. W., DePoy, D. L., Marshall, J. L., Stanek, K. Z., Stutz, A. M., Poindexter, S., Siverd, R., O'Brien, T. P., Trueblood, M., and Trueblood, P. (2007). The Kilo-degree Extremely Little Telescope (KELT): A Small Robotic Telescope for Large-Area Synoptic Surveys. *PASP*, 119:923–935.

Pepper, J., Rodriguez, J. E., Collins, K. A., Johnson, J. A., Fulton, B. J., Howard, A. W., Beatty, T. G., Stassun, K. G., Isaacson, H., Colón, K. D., Lund, M. B., Kuhn, R. B., Siverd, R. J., Gaudi, B. S., Tan, T. G., Curtis, I., Stockdale, C., Mawet, D., Bottom, M., James, D., Zhou, G., Bayliss, D., Cargile, P., Bieryla, A., Penev, K., Latham, D. W., Labadie-Bartz, J., Kielkopf, J., Eastman, J. D., Oberst, T. E., Jensen, E. L. N., Nelson, P., Sliski, D. H., Wittenmyer, R. A., McCrady, N., Wright, J. T., Relles, H. M., Stevens, D. J., Joner, M. D., and Hintz, E. (2017). KELT-11b: A Highly Inflated Sub-Saturn Exoplanet Transiting the V = 8 Subgiant HD 93396. *AJ*, 153:215.

Perna, R., Menou, K., and Rauscher, E. (2010). Ohmic Dissipation in the Atmospheres of Hot Jupiters. *ApJ*, 724:313–317.

Perryman, M. (2014). *The Exoplanet Handbook*.

Perryman, M., Hartman, J., Bakos, G. Á., and Lindegren, L. (2014). Astrometric Exoplanet Detection with Gaia. *ApJ*, 797:14.

Piskorz, D., Benneke, B., Crockett, N. R., Lockwood, A. C., Blake, G. A., Barman, T. S., Bender, C. F., Bryan, M. L., Carr, J. S., Fischer, D. A., Howard, A. W., Isaacson, H., and Johnson, J. A. (2016). Evidence for the Direct Detection of the Thermal Spectrum of the Non-Transiting Hot Gas Giant HD 88133 b. *ApJ*, 832:131.

Piskorz, D., Benneke, B., Crockett, N. R., Lockwood, A. C., Blake, G. A., Barman, T. S., Bender, C. F., Carr, J. S., and Johnson, J. A. (2017). Detection of Water Vapor in the Thermal Spectrum of the Non-transiting Hot Jupiter Upsilon Andromedae b. *AJ*, 154:78.

Pollacco, D. L., Skillen, I., Collier Cameron, A., Christian, D. J., Hellier, C., Irwin, J., Lister, T. A., Street, R. A., West, R. G., Anderson, D. R., Clarkson, W. I., Deeg, H., Enoch, B., Evans, A., Fitzsimmons, A., Haswell, C. A., Hodgkin, S., Horne, K., Kane, S. R., Keenan, F. P., Maxted, P. F. L., Norton, A. J., Osborne, J., Parley, N. R., Ryans, R. S. I., Smalley, B., Wheatley, P. J., and Wilson, D. M. (2006). The WASP Project and the SuperWASP Cameras. *PASP*, 118:1407–1418.

Pollack, J. B., Hubickyj, O., Bodenheimer, P., Lissauer, J. J., Podolak, M., and Greenzweig, Y. (1996). Formation of the Giant Planets by Concurrent Accretion of Solids and Gas. *Icarus*, 124:62–85.

Rodler, F., Kürster, M., and Barnes, J. R. (2013). Detection of CO absorption in the atmosphere of the hot Jupiter HD 189733b. *MNRAS*, 432:1980–1988.

Rodler, F., Lopez-Morales, M., and Ribas, I. (2012). Weighing the Non-transiting Hot Jupiter τ Boo b. *ApJ*, 753:L25.

Schwartz, J. C. and Cowan, N. B. (2015). Balancing the energy budget of short-period giant planets: evidence for reflective clouds and optical absorbers. *MNRAS*, 449:4192–4203.

Schwarz, H., Ginski, C., de Kok, R. J., Snellen, I. A. G., Brogi, M., and Birkby, J. L. (2016). The slow spin of the young substellar companion GQ Lupi b and its orbital configuration. *A&A*, 593:A74.

Sedaghati, E., Boffin, H. M. J., MacDonald, R. J., Gandhi, S., Madhusudhan, N., Gibson, N. P., Oshagh, M., Claret, A., and Rauer, H. (2017). Detection of titanium oxide in the atmosphere of a hot Jupiter. *Nature* , 549:238–241.

Sing, D. K., Fortney, J. J., Nikolov, N., Wakeford, H. R., Kataria, T., Evans, T. M., Aigrain, S., Ballester, G. E., Burrows, A. S., Deming, D., Désert, J.-M., Gibson, N. P., Henry, G. W., Huitson, C. M., Knutson, H. A., Lecavelier Des Etangs, A., Pont, F., Showman, A. P., Vidal-Madjar, A., Williamson, M. H., and Wilson, P. A. (2016). A continuum from clear to cloudy hot-Jupiter exoplanets without primordial water depletion. *Nature* , 529:59–62.

Snellen, I. A. G., Brandl, B. R., de Kok, R. J., Brogi, M., Birkby, J., and Schwarz, H. (2014). Fast spin of the young extrasolar planet β Pictoris b. *Nature* , 509:63–65.

Snellen, I. A. G. and Brown, A. G. A. (2018). The mass of the young planet Beta Pictoris b through the astrometric motion of its host star. *Nature Astronomy*.

Snellen, I. A. G., de Kok, R. J., de Mooij, E. J. W., and Albrecht, S. (2010). The orbital motion, absolute mass and high-altitude winds of exoplanet HD209458b. *Nature* , 465:1049–1051.

Snellen, I. A. G., Stuik, R., Navarro, R., Bettonvil, F., Kenworthy, M., de Mooij, E., Otten, G., ter Horst, R., and le Poole, R. (2012). Ground-based search for the brightest transiting planets with the Multi-site All-Sky CAmeRA: MASCARA. In *Ground-based and Airborne Telescopes IV*, volume 8444 of *Proc. SPIE*, page 84440I.

Steffen, J. H., Fabrycky, D. C., Agol, E., Ford, E. B., Morehead, R. C., Cochran, W. D., Lissauer, J. J., Adams, E. R., Borucki, W. J., Bryson, S., Caldwell, D. A., Dupree, A., Jenkins, J. M., Robertson, P., Rowe, J. F., Seader, S., Thompson, S., and Twicken, J. D. (2013). Transit timing observations from Kepler - VII. Confirmation of 27 planets in 13 multiplanet systems via transit timing variations and orbital stability. *MNRAS*, 428:1077–1087.

Stuik, R., Bailey, J. I., Dorval, P., Talens, G. J. J., Laginja, I., Mellon, S. N., Lomberg, B. B. D., Crawford, S. M., Ireland, M. J., Mamajek, E. E., and Kenworthy, M. A. (2017). bRing: An observatory dedicated to monitoring the β Pictoris b Hill sphere transit. *A&A*, 607:A45.

Valenti, J. A. and Fischer, D. A. (2005). Spectroscopic Properties of Cool Stars (SPOCS). I. 1040 F, G, and K Dwarfs from Keck, Lick, and AAT Planet Search Programs. *ApJS*, 159:141–166.

Vogt, S. S., Marcy, G. W., Butler, R. P., and Apps, K. (2000). Six New Planets from the Keck Precision Velocity Survey. *ApJ*, 536:902–914.

Winn, J. N., Fabrycky, D., Albrecht, S., and Johnson, J. A. (2010). Hot Stars with Hot Jupiters Have High Obliquities. *ApJ*, 718:L145–L149.

Wolszczan, A. and Frail, D. A. (1992). A planetary system around the millisecond pulsar PSR1257 + 12. *Nature* , 355:145–147.

Wright, J. T., Marcy, G. W., Howard, A. W., Johnson, J. A., Morton, T. D., and Fischer, D. A. (2012). The Frequency of Hot Jupiters Orbiting nearby Solar-type Stars. *ApJ*, 753:160.

Wu, Y. and Lithwick, Y. (2013). Ohmic Heating Suspends, Not Reverses, the Cooling Contraction of Hot Jupiters. *ApJ*, 763:13.